Published online 26 September 2016

Nucleic Acids Research, 2017, Vol. 45, No. 1 ***181–197***
doi: 10.1093/nar/gkw850

SAC3B, a central component of the mRNA export complex TREX-2, is required for prevention of epigenetic gene silencing in *Arabidopsis*

Yu Yang[1,2,3], Honggui La[1,4], Kai Tang[2], Daisuke Miki[1], Lan Yang[1], Bangshing Wang[2], Cheng-Guo Duan[2], Wenfeng Nie[1], Xingang Wang[2], Siwen Wang[5], Yufeng Pan[1], Elizabeth J. Tran[5], Lizhe An[3], Huiming Zhang[1,6,*] and Jian-Kang Zhu[1,2,6,*]

[1]Shanghai Center for Plant Stress Biology, Shanghai Institutes of Biological Sciences, Chinese Academy of Sciences, Shanghai 201602, China, [2]Department of Horticulture and Landscape Architecture, Purdue University, West Lafayette, IN 47907, USA, [3]Ministry of Education Key Laboratory of Cell Activities and Stress Adaptations, School of Life Sciences, Lanzhou University, Lanzhou, Gansu 730000, China, [4]Department of Biochemistry and Molecular Biology, Nanjing Agricultural University, Nanjing, Jiangsu 210095, China, [5]Department of Biochemistry, Purdue University, West Lafayette, IN 47906, USA and [6]CAS Center for Excellence in Molecular Plant Sciences, Shanghai Institutes of Biological Sciences, Chinese Academy of Sciences, Shanghai 201602, China

Received June 12, 2016; Revised September 05, 2016; Accepted September 07, 2016

ABSTRACT

Epigenetic regulation is important for organismal development and response to the environment. Alteration in epigenetic status has been known mostly from the perspective of enzymatic actions of DNA methylation and/or histone modifications. In a genetic screen for cellular factors involved in preventing epigenetic silencing, we isolated an Arabidopsis mutant defective in SAC3B, a component of the conserved TREX-2 complex that couples mRNA transcription with nuleo-cytoplasmic export. Arabidopsis SAC3B dysfunction causes gene silencing at transgenic and endogenous loci, accompanied by elevation in the repressive histone mark H3K9me2 and by reduction in RNA polymerase Pol II occupancy. SAC3B dysfunction does not alter promoter DNA methylation level of the transgene *d35S::LUC*, although the DNA demethylase ROS1 is also required for *d35S::LUC* anti-silencing. THP1 and NUA were identified as SAC3B-associated proteins whose mutations also caused *d35S::LUC* silencing. RNA-DNA hybrid exists at the repressed loci but is unrelated to gene suppression by the *sac3b* mutation. Genome-wide analyses demonstrated minor but clear involvement of SAC3B in regulating siRNAs and DNA methylation, particularly at a group of TAS and TAS-like loci. Together our results revealed not only a critical role of mRNA-export factors in transcriptional anti-silencing but also the contribution of SAC3B in shaping plant epigenetic landscapes.

INTRODUCTION

Epigenetic silencing is important for gene regulation during development and for the inactivation of viruses, transposons and transgenes (1,2). Transcription activity depends on chromatin status that is characterized by epigenetic marks including DNA methylation and histone modifications. In plants, DNA methylation at the fifth position of cytosine is found in CG, CHG and CHH contexts (H is A, T or C). *De novo* methylation can be mediated through the RNA-directed DNA methylation (RdDM) pathway (3). Maintenance of CG methylation is catalyzed by MET1, which recognizes a semi-methylated ^{me}CG/GC during DNA replication and methylates the unmodified cytosine; whereas CHG methylation is maintained by CMT3, which is a plant specific methyltransferase (4). The asymmetric CHH methylation is maintained through persistent *de novo* methylation catalyzed by DRM2 through the RdDM pathway, and by CMT2 that requires the chromatin remodeling protein DDM1 (5,6).

Besides DNA methylation, histone modifications and chromatin remodeling are also important factors that affect epigenetic status (4,7). Dimethylation at Histone H3 Lys9 (H3K9me2) is a typical repressive epigenetic mark which is deposited by Su(var)3-9 homologs and is closely related to DNA methylation (8). A combination of DNA methylation and H3K9me2 marks in gene promoter often causes repressed gene expression (9,10). On the other hand, anti-

*To whom correspondence should be addressed. Tel: +86 21 57078277; Fax: +86 21 57078213; Email: hmzhang@sibs.ac.cn
Correspondence may also be addressed to Jian-Kang Zhu. Tel: +86 21 57078201; Fax: +86 21 57078213; Email: jkzhu@sibs.ac.cn

silencing mechanisms exist to counteract epigenetic silencing. Active DNA demethylation is an important way to prevent the spreading of methylation from repetitive sequences to neighboring genes (11). In *Arabidopsis*, a family of 5-methylcytosine DNA glycosylases including ROS1, DME, DML2 and DML3 enzymatically remove DNA methylation to prevent genes from being silenced (4,12). Release of transcriptional gene silencing can also occur without changing DNA methylation, as exemplified by the *Arabidopsis mom1* mutant, in which transcriptional silencing was released through an unknown mechanism without alteration in DNA methylation levels (13). Recently, additional cellular anti-silencing factors have been identified that helps to reveal multiple mechanisms through which genes are protected from epigenetic silencing (14,15).

Eukaryotic RNA polymerase II transcription produces pre-mRNAs that are subjected to an array of processing events including capping at the 5′ end, splicing, cleavage and polyadenylation at the 3′ end and export to the cytoplasm (16). In *S. cerevisiae*, mRNA nucleo-cytoplasmic export involves a variety of conserved factors, including the TREX (transcription/export) complex, the export receptor Mex67-Mtr2 and the TREX-2 complex (17). TREX associates with nascent transcripts during transcription elongation, facilitating mRNP formation and recruitment of additional RNA-binding proteins (17–19). The heterodimeric Mex67-Mtr2 interacts with Phe-Gly (FG)-rich nucleoporins and facilitates RNA export through transport channel of the nuclear pore complex (17,20). The TREX-2 complex, which consists of Sac3, Thp1, Sus1, Cdc31 and Sem1, anchors the transcribed genes to nuclear pore complex (NPC) through NPC-TREX-2 interaction (21–24). In *S. cerevisiae,* defective TREX-2 disrupts transcription elongation and causes transcription-dependent hyper-recombination (25). Mutations in yeast TREX-2 complex also lead to co-transcriptional accumulation of DNA:RNA hybrid (i.e. R-loop) that was shown to impair transcription *in vitro* (25,26). In Arabidopsis, the TREX complex was reported to be involved in siRNA biogenesis (27). It was also found that HPR1 of the TREX complex controls transcription of the gene *RTE1* (REVERSION-TO-ETHYLENE SENSITIVITY1) (28). In contrast, limited information is available for the function of the TREX-2 complex in plants. While a functional TREX-2 complex may also exist in Arabidopsis (29), it is unknown how Arabidopsis TREX-2 complex may affect gene expression. It is also unclear, particularly on a whole-genome scale, how a functional TREX-2 complex may be involved in production of small interfering RNAs (siRNAs) and epigenetic regulation.

The largest subunit of the TREX-2 complex is SAC3 that acts as a central scaffold for the whole protein complex (30). Here, we report isolation of an Arabidopsis *sac3* mutant. With the goal to identify anti-silencing factors in Arabidopsis, we performed a forward genetic screen using a transgenic reporter line previously named YJ, which harbors a luciferase reporter gene driven by double 35S (*d35S*) promoter (31). One mutant with decreased luminescence was subjected for further study, and the mutation was mapped to the gene of SAC3B, an Arabidopsis homolog of yeast SAC3. Silencing of the transgene *d35S::LUC* is accompanied by increased H3K9me2 mark and decreased Pol II occupancy, but not increased DNA methylation nor increased R-loop accumulation. SAC3B physically associates with THP1 and NUA, two proteins that are also involved in mRNA export. Mutations in THP1 and NUA also cause gene silencing, indicating that Arabidopsis mRNA export components including the TREX-2 complex affects transcription in addition to mRNA nucleo-cytoplasmic transport. In addition, our genome-wide analyses revealed a contribution of SAC3B in Arabidopsis epigenetic regulation.

MATERIALS AND METHODS

Plant materials and growth conditions

The wild type in this study refers to the transgenic plant previously named YJ (31), which contains two transgenes, *d335S::LUC* and *d35S::NPTII*, in the *rdr6-11* background (31). EMS mutagenesis of the wild type was conducted as described previously (31). Mutants with reduced luminescence, based on the luciferase live imaging, were isolated from M2 generation. *p31* and *ros1-18* mutant were both obtained from this screening. The *ros1-18* mutant contains a point mutation from G_{1961} to A, resulting in the amino acid change from Trp_{533} to a premature stop codon. The T-DNA insertion mutants *nrpd1a-3* (SALK_128428), *sac3b-7* (SALK_111245), *sac3b-3* (SALK_065672), *thp1-1* (SAIL_82_A02) and *nua-3* (SAIL_505_H11) were obtained from the Arabidopsis Biological Resource Center. All Arabidopsis plants were in Col-0 genetic background unless stated otherwise.

Seeds were sowed on half-strength Murashige and Skoog (MS) media containing 1.5% sucrose with 0.7% (for horizontal plate) or 1% (for vertical plate) agar. After stratification at 4°C for 2 days, plants were grown under a long day photoperiod (16 h light/8 h dark) at 22°C. For kanamycin or 5-Aza-2′-deoxycytodine (5′az-2′c) treatment, seeds were sowed on half-strength MS media plus 1.5% sucrose and 0.7% agar supplemented with 160 mg/l Kanamycin or 7 μg/ml 5az-2′c (Sigma, A3656), respectively, and subsequently grown for 12 days before imaging.

Luciferase live imaging

For luciferase live imaging, seedlings were grown on plates with half-strength MS media supplemented with 0.7% agar and 1.5% sucrose. Ten to twelve-day-old seedlings were sprayed with 1 mM luciferin (PerkinElmer, Cat. 122796) in 0.01% Triton X-100. After 10 min incubation in the dark, the plants were placed in a Princeton Dark Box equipped with a Roper VersArray1300B camera controlled by the WinView32 software, and then imaged with a 5 min exposure time.

Quantitative real time PCR

RNA was extracted from 12-day-old seedlings by Trizol (invitrogen) method followed by DNase (Turbo) treatment. For mRNA expression analysis, 1 μg total RNA was used for reverse transcription by oligo dT using SuperscriptIII RT kit (invitrogen) according to the manufacturer's instructions. For *COOLAIR* expression analysis, gene specific

primer (set6_LP) described previously was used for reverse transcription and total *FLC* antisense RNA was assayed (32). Real-time PCR was carried out using iQ SYBR Green Supermix (Biorad) on a CFX96 real-time PCR detection system (Bio-RAD). A housekeeping gene, *TUB8,* was used as the internal control for all reactions. The fold change of gene expression value was calculated as described previously (31). All primers were listed in Supplementary Table S1.

Bisulfite sequencing of individual loci

Bisulfite sequencing of individual loci was conducted as described previously (33). Two hundred nanograms of genomic DNA were treated with the BisulFlash DNA Modification Kit (Epigentek) following the manufacturer's protocols. Three microliters of bisulfite-treated DNA was used for each PCR assay (in 20 μl final volume) using ExTaq (Takara) with primers specific to the corresponding regions (Supplementary Table S1). PCR products were cloned into the pGEM-T easy vector (Promega) following the supplier's instructions. Twenty independent clones for each sample were sequenced and analyzed using the online tool CyMATE (http://www.cymate.org/) (34).

Map-based cloning

The *p31* mutant in the Col-0 background was crossed to wild-type YJ in Landsberg background (31). The resulting F1 seeds were selfed to produce the F2 population, from which plants showing low transgenic luciferase (LUC) phenotype were selected as the mapping population. Rough mapping using 40 F2 plants localized the mutation at the top of the chromosome 3 between markers CL301_B8M1 (position 1583.06K) and CL302_B8M1 (position2491.99K). Further mapping based on 256 F2 plants delimited the mutation to an interval of about 280K between markers CL301_B11M1 (position 1800.297K) and CL302_B3M2 (position 2087.074K). Then the *p31* mutant genome was sequenced to search the mutations in this mapping interval. Sequences of the mapping primers were provided in Supplementary Table S1.

Plasmid construction and SAC3B complementation

SAC3B genomic sequence including a 1923 bp promoter region was amplified and cloned into pCAMBIA1305-C-3XFlag-nos and pCAMBIA1305-C-3XMYC-nos, between the Kpn1 and Xba1 restriction sites. The construction was confirmed by sequencing, transformed into *Agrobacterium tumefaciens* strain GV3101 and later transformed into the *p31* mutant via floral dipping method.

Chromatin immunoprecipitation assays

Three grams of 12-day-old seedlings of WT and *p31* mutant was harvested and the chromatin immunoprecipitation (ChIP) assays were performed as described previously (35). The antibodies were anti-Histone H3 (di methyl K9) antibody (ab1220, abcam), anti-RNA polymerase II CTD repeat YSPTSPS [8WG16] antibody (ab817, abcam) and anti-monomethyl-Histone H3 (Lys27) antibody (07-448, millipore). Primers used in qPCR are listed in Supplementary Table S1.

R-loop foot-printing

R-loop foot-printing experiment was performed as described previously with minor modification (36). Briefly, 3g of 13-day-old seedlings are grind into powder in liquid nitrogen. Nuclei were purified in Honda buffer (0.44 M Sucrose, 1.25% Ficoll, 2.5% Dextran T40, 20 mM Hepes KOH pH7.4, 10 mM MgCl2, 0.5% Triton X-100, 5 mM DTT, protease Inhibitors), and treated with proteinase K (Ambion) at 37°C overnight. DNA was purified by PCI (25:24:1, sigma, PH8.0). A total of 1.5 μg DNA was subjected to sodium bisulfite treatment at 37°C overnight, and was cleaned up using EZ DNA methylation Gold Kit Cat (Zymo). *d35S::LUC* strand-specific PCR was performed using sense-1/2R and sense-2F/3 primer pairs (for sense strand), and anti-1/2R primer pairs (for antisense strand), respectively. *FLC* antisense stand-specific PCR was performed by FLC-1/2R (36). The PCR products were gel-extracted and cloned into pEasy-T3 vector (Transgene). Individual colonies were sent for sequencing. The sequencing results were analyzed by the online tool Kismeth (37).

DNA IP assay

DNA immunoprecipitation (DNA IP) assays were performed according to Sun *et al.* with minor modifications (36). Briefly, 3g of 12-day-old seedlings of WT and *p31* mutant were harvested, and crosslinked in phosphate buffered saline (PBS) containing 0.5% formaldehyde. Nuclei were purified in Honda buffer with protease Inhibitors (Sigma, P9599) and RNase inhibitor (Invitrogen, AM2684). The nuclei was resuspended in 500 μl Nuclei lysis buffer (50 mM Tris-HCl, pH8.0, 10 mM EDTA, 1% SDS, protease Inhibitors and RNase inhibitor) and sonicated by a sonicator (Bioruptor UCD-200) at high power for a total time of 30 min (working for 15 s then pause for 30 s). After resuspension and sonication, the samples were centrifuged at 4°C and the supernatant was diluted with 400 μl Elution buffer (1% SDS, 0.1 M $NaHCO_3$) into each 100 μl chromatin extraction. Reverse crosslink with RNase inhibitor was performed overnight, followed by proteinase K (Fermentas) digestion for 1.5 h at 45°C to remove proteins. Total nucleic acid (TNA) was extracted using equal volume of phenol/chloroform/isoamyl alcohol (25:24:1, sigma), and was dissolved in 50 μl water. For negative control, 1 μg TNA was subjected to RNase H (New England Biolabs) treatment at 37°C for 2 h. For IP, the Dynabeads were washed and diluted 10 times with Chip binding/washing buffer (150 mM NaCl, 20 mM Tris-HCl pH8, 2 mM EDTA, 1%Triton X-100 and 0.1% SDS) before use. One microgram TNA was diluted to 1 ml in ChIP dilution buffer (1.1% Triton X-100, 1.2 mM EDTA, 16.7 mM TrisHCl pH8.0 and 167 mM NaCl), and precleared by incubation with 50 μl diluted Dynabeads at 4°C for 2 h with gentle rotation. At the same time, 100 μl diluted Dynabeads was conjugated with S9.6 antibody at 4°C for 2 h with gentle rotation. After preclearing and conjugation, the precleared sample solution

was transferred into the Dynabeads conjugated with the S9.6 antibody. IP was performed overnight at 4°C with gentle rotation. The beads were then washed at 4°C with Chip Binding/Washing Buffer twice, with TE buffer (10 mM Tris-HCl pH8.0, 1 mM EDTA) twice, and then eluted with 250 μl Elution buffer twice. DNA was extracted from the elution by equal volume of PCI (25:24:1) and precipitated. The pellet was dissolved in 50 μl water, from which 3 μl was used for each qPCR reaction. Primers used in qPCR were listed in Supplementary Table S1.

Affinity purification and mass spectrometry

The IP and affinity purification were performed as described previously with minor modifications (38). Briefly, ∼2 g of flower tissue collected from SAC3B-3XFlag transgenic T4 plants were ground to a fine powder in liquid nitrogen and suspended in 15 ml of lysis buffer (50 mM Tris [pH 7.6], 150 mM NaCl, 5 mM MgCl2, 10% glycerol, 0.1% NP-40, 0.5 mM DTT, 1 mg/ml pepstatin, 1 mM PMSF and 1% protease inhibitor cocktail [Sigma, P9599]). The tissue was further homogenized by douncing and then centrifuged at 4°C for 25 min at 12 500 rpm. Eighty microliters of Dynabeads (Invitrogen, 10003D) that had been conjugated with Flag antibody (Sigma, F1804) according to the manufacturer's instructions were added to the supernatant for IP. After incubation at 4°C with rotation for 2.5 h, the Flag beads were washed once with 5 ml of LB for 15 min, and then 5 times for 5 min with 1 ml of LB, and twice for 5 min with 1 ml PBS. The protein was then subjected to Mass Spectrometry analysis according to previously described procedures (15).

Whole genome bisulfite sequencing and data analysis

Twelve-day-old seedlings of Col-0, *sac3b-7* and *sac3b-3* were used for extraction of genomic DNA using Qiagen DNeasy Plant mini kit. Bisulfite conversion, library construction and deep sequencing were performed by the Core Facility of Genomics in Shanghai Plant Stress Biology Center, China. The *nrpd1a-3* and *nrpd1b-11* data was from previously published data (39).

For data analysis, low quality sequences (q < 20) were trimmed using *trim in BRAT-BW* (40) and clean reads were mapped to the TAIR10 genome using BRAT-BW and allowing two mismatches. To remove potential PCR duplicates, the remove-dupl command of BRAT-BW was used. Differentially methylated regions (DMRs) were identified according to (41). In brief, only cytosines with at least 4X coverage in all libraries in the same background were considered. A sliding-window approach with a 200-bp window sliding at 50-bp intervals was used to identify DMRs. Fisher's exact test was performed for methylated versus unmethylated cytosines for each context, within each window, with FDRs estimated using a Benjamini–Hochberg adjustment of Fisher's *P*-values calculated in the R environment. Windows with an FDR ≤ 0.05 were considered for further analysis, and windows within 100 bp of each other were condensed to larger regions. Regions were then adjusted to extend to differentially methylated cytosines (DMCs) at each border. A cytosine was considered differentially methylated if it showed at least a 2-fold change in methylation percentage in the mutant. The regions were then filtered to include only those with at least 10 DMCs and with at least an average of a 2-fold change in methylation percentage per cytosine.

mRNA-seq and data analysis

Total RNA were extracted from 12-day-old seedlings of Col-0 and *sac3b-7* using Trizol reagent (Ambion, 15596) and treated with DNase (Turbo) to remove any genomic DNA contaminants. Each sample has two biological replicates. Library construction and deep sequencing were performed by the Core Facility of Genomics in Shanghai Plant Stress Biology Center, China. Clean reads, from which the adapters and low-quality sequences were removed, were mapped to the TAIR10 genome by program TopHat2 (42), allowing up to two mismatches. Only uniquely mapped reads were retained for downstream analysis. Htseq-count (43) was used to get the read counts for each gene. Differentially expressed genes were identified by edgeR (44) with cut-off as fold change >2 and FDR < 0.05. The gene ontology (GO) enrichment analysis was performed by the online tool agriGO (http://bioinfo.cau.edu.cn/agriGO/) (45).

Small RNA sequencing and data analysis

Total RNA was extracted from 12-day-old seedlings of Col-0, *sac3b-7* and *sac3b-3* mutants using Trizol reagent. Library construction and deep sequencing were performed by the Beijing Genomics Institute in Shenzhen, China. The *nrpd1a-3* data were from previously published data (39). Analyses of small RNA (sRNA) data were conducted according to (39) with minor modifications. Briefly, after adapter sequences were trimmed, clean reads were mapped to the TAIR10 genome and annotated structural RNAs (rRNAs, tRNAs, snRNAs and snoRNAs) using Bowtie (46). Only sRNAs that had at least one perfect match to the genome and did not match structural RNAs were used for downstream analysis. Read counts were normalized to reads per 10 million (RPTM) according to total number of clean reads (excluding structural sRNAs) in the library and number of hits to the genome. Normalized expression levels of 21 or 24-nt sRNAs were summarized in non-overlapping 500-nt windows over the nuclear genome and were compared between each mutant and the wild type. To remove lowly expressed regions, only 500-nt regions that had at least 100 RPTM combined expression in the mutant and the wild type were considered.

RESULTS

Isolation of the *p31* mutant with gene silencing and growth impairment phenotypes

In an effort to identify anti-silencing factors, we screened an EMS-generated mutant pool, which was derived from a transgenic Arabidopsis line named YJ carrying a luciferase-based reporter of transcriptional gene silencing (31). In this reporter system, the LUC expression is under control of a double *35S* promoter (*d35S*) where DNA methylation is present and thus is subjected to epigenetic regulation

(31). We identified a mutant that showed a LUC silencing phenotype and named it *p31*. Compared to the original transgenic plant YJ (hereafter referred to as WT), *p31* displayed lower luminescence (Figure 1A), similar to the newly isolated *ros1-18* mutant that harbors a null mutation in the DNA demethylase ROS1, a known anti-silencing factor. Consistent with the phenotype of reduced LUC signals, *p31* showed decreased transcript level of *d35S::LUC* (Figure 1B). The *p31* mutant also showed gene silencing of *d35S::NPTII*, which is another transgene that confers plant resistance to kanamycin (Figure 1A and B). We examined *ROS1* gene expression in the *p31* mutant. The results showed that *ROS1* expression is unaffected by the mutation in *p31* (Figure 1B), indicating that gene silencing phenotypes in *p31* is not caused indirectly through *ROS1* down-regulation. In the wild type control for *p31*, curly leaves were observed due to *rdr6-11* mutation (47), whereas *p31* displayed severer curly leaf phenotype compared to the wild type control (Figure 1C). Moreover, the *p31* mutant plants additionally exhibited multiple phenotypes of impaired growth, including shorter primary roots, fewer lateral roots, smaller leaves and shorter inflorescence (Figure 1C), indicating an important role of this gene in plant growth and development.

The *p31* mutant shows transcriptional silencing of the transgene

Silencing of *d35S::LUC* can be suppressed by inhibition of DNA methylation, as demonstrated by the increased LUC signals in *p31* and *ros1-18* plants treated with 5-aza-2′-deoxycytidine, which is a DNA methylation inhibitor (Figure 2A). To test whether *d35S::LUC* gene silencing in *p31* results from promoter DNA hypermethylation, we compared DNA methylation levels in *p31* and WT by performing bisulfite sequencing. Within the examined *d35S::LUC* region, cytosines in the asymmetric CHH context are the majority among all cytosines in both the top and the bottom strands. The *p31* mutant displayed similar DNA methylation levels compared to WT in all three cytosine contexts (CG, CHG and CHH). Such a pattern was observed in both the top and the bottom strands (Figure 2B). In contrast, the *ros1-18* mutant showed hypermethylation in both strands compared with WT, especially in the CG context (Figure 2B). ChIP analyses revealed that *d35S* promoter in *p31* accumulated higher levels of H3K9me2, which is a histone mark repressive to RNA polymerase Pol II (Figure 2C). Consistent with the increased heterochromatic histone mark at *d35S* promoter in *p31*, chromatin occupancy of Pol II at *d35S* promoter region was decreased in *p31* compared to WT (Figure 2C), supporting that *p31* mutation results in transcriptional gene silencing.

SAC3B dysfunction is responsible for the *p31* mutant phenotypes

Backcrossing of *p31* to WT resulted in F1 plants that all exhibited a wild-type luminescence phenotype, while the selfed F2 progenies segregated approximately 3:1 for wild type versus mutant based on LUC phenotype, indicating the mutation of interest is recessive and in a single nuclear gene. As a result of genetic mapping combined with whole genome sequencing, we identified a single nucleotide substitution in the *SAC3B* (At3g06290) gene in *p31* mutant. The mutation from CAA to TAA is predicted to change Gln-162 to a premature stop codon (Supplementary Figure S1).

To confirm that *p31* mutant phenotypes were caused by *sac3b* mutation, complementation of *p31* was performed by transgenic expression of a wild-type *SAC3B* gene driven by its native promoter. Two differently epitode-tagged genomic clones, *SAC3Bp::SAC3B-3MYC* and *SAC3Bp::SAC3B-3FLAG*, both restored LUC signals in *p31* back to WT level (Figure 3A). Consistently, *LUC* gene expression was rescued in *SAC3Bp::SAC3B-3MYC* and *SAC3Bp::SAC3B-3FLAG* transgenic lines, so was the other transgene *d35S::NPTII* (Figure 3B). In addition, *p31* phenotypes of growth retardation including shorter primary roots, fewer lateral roots, smaller and curly leaves and shorter inflorescence were also rescued in the complementation lines (Figure 3C). Furthermore, two SAC3B T-DNA insertion lines, *sac3b-7* and *sac3b-3*, showed morphological phenotypes similar to those observed in *p31* (Supplementary Figure S2). Taken together, these results demonstrate that SAC3B is the gene responsible for transcriptional silencing and morphological phenotypes of *p31*.

Mutations in other mRNA export components cause *d35S::LUC* silencing

Because SAC3B is a key component of the mRNA export complex TREX-2, we asked if mutations in other components in mRNA export pathway are also able to silence the *d35S::LUC* transgene. We used transgenic plants with epitope-tagged SAC3B driven by its native promoter, and performed co-immunoprecipitation followed by mass spectrometry analysis (IP-MS) to search for SAC3B-associated proteins. THP1, another known component of the TREX-2 mRNA export complex (29), was identified in each of the four biological replicates of our IP-MS experiments (Figure 4A). We next introduced *d35S:LUC* transgene into the *thp1-1* mutant by genetic crossing with WT plants that harbor *d35S::LUC*. Homozygous *thp1-1 d35S::LUC* mutants strongly exhibited defective growth phenotypes such as smaller and curly leaves and shorter inflorescence (Supplementary Figure S3B). Nevertheless, reduced LUC luminescence was observed in mature leaves of homozygous *thp1-1* mutant plants carrying the *d35S:LUC* transgene (Figure 4B). Consistently, RT-qPCR results showed that transcript levels of *LUC* and *NPTII* were decreased in *thp1-1 d35SLUC* plants (Figure 4C). These results indicate that gene silencing in *sac3b* and *thp1-1* mutants is due to dysfunction of the TREX-2 mRNA export complex.

In addition to THP1, Nuclear Pore Anchor (NUA) that is known to be involved in nuclear pore-associated mRNA export in plants, was also repetitively identified as a SAC3B-interacting protein by our IP-MS analyses (Figure 4A). The *nua-3* mutant showed defective growth phenotypes such as reduced leaf size and early flowering as was reported previously (48). Similar to SAC3B and THP1, NUA mutation also leads to gene silencing, as shown by the repressed gene expression of *d35S::LUC* in the *nua-3* mutant background (Figure 4B and C). Moreover, the transgene repres-

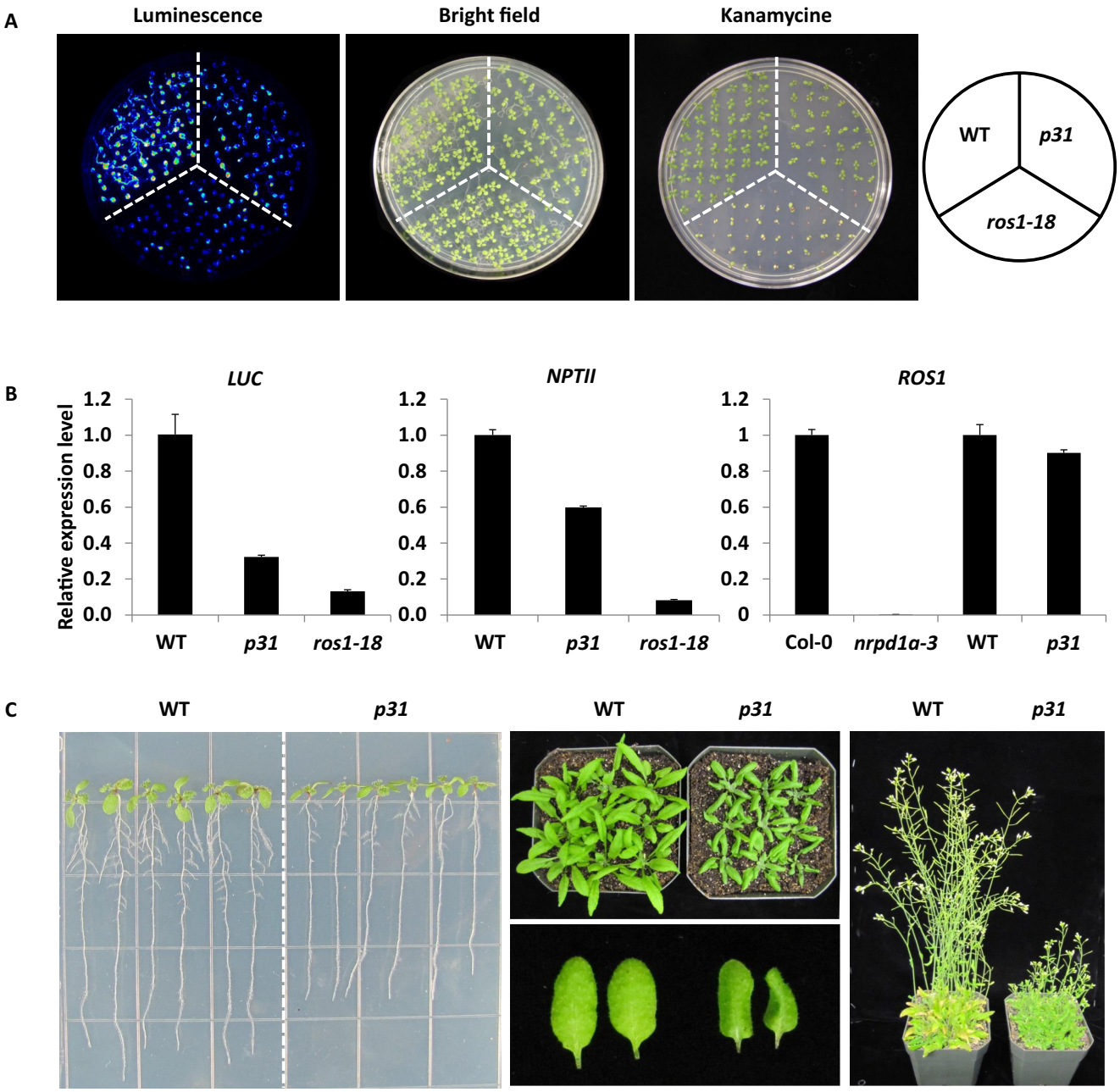

Figure 1. Gene silencing and impaired growth phenotypes in the *p31* mutant. (**A**) The *p31* and *ros1-18* mutant displayed reduced luminescence signals and kanamycin resistance, which indicated gene expression levels of *d35S::LUC* and *d35S::NPTII*, respectively. (**B**) Analyses of *LUC*, *NPTII* and *ROS1* gene expression levels by quantitative real time PCR. For *ROS1* expression level, the *nrpd1a-3* mutant in which ROS1 is known to be repressed was used as a control. *TUB8* expression levels were used for normalization. Error bars indicate SEM from three biological replicates. (**C**) Morphological phenotypes of *p31* mutants including shorter root length, less lateral root, curly leaves and reduced height.

sion in *nua-3-d35S::LUC* mutant was also accompanied by increased H3K9 di-methylation and decreased Pol II occupancy at the promoter region (Supplementary Figure S3C and D). Unlike H3K9me2, another repressive histone mark H3K27me was not affected by mutations in either *p31* or *nua-3-d35S::LUC* plants at the *d35S* promoter (Supplementary Figure S3E). Together, our results show that dysfunction in mRNA export factors causes *d35S::LUC* silencing in Arabidopsis.

Effects of *sac3b* mutation on expression of endogenous genes

To assess the genome-wide effects of SAC3B mutation on *Arabidopsis* gene transcription, we carried out mRNAseq to profile transcriptomes in *sac3b-7* and Col-0. The *sac3-7* mutant showed a total of 624 differentially expressed genes (DEGs) (Fold change $>$ 2, FDR $<$ 0.05), among which 276 were up-regulated and 348 were down-regulated compared to Col-0. GO analysis revealed that the up-regulated genes are mainly involved in cellular biosynthetic processes,

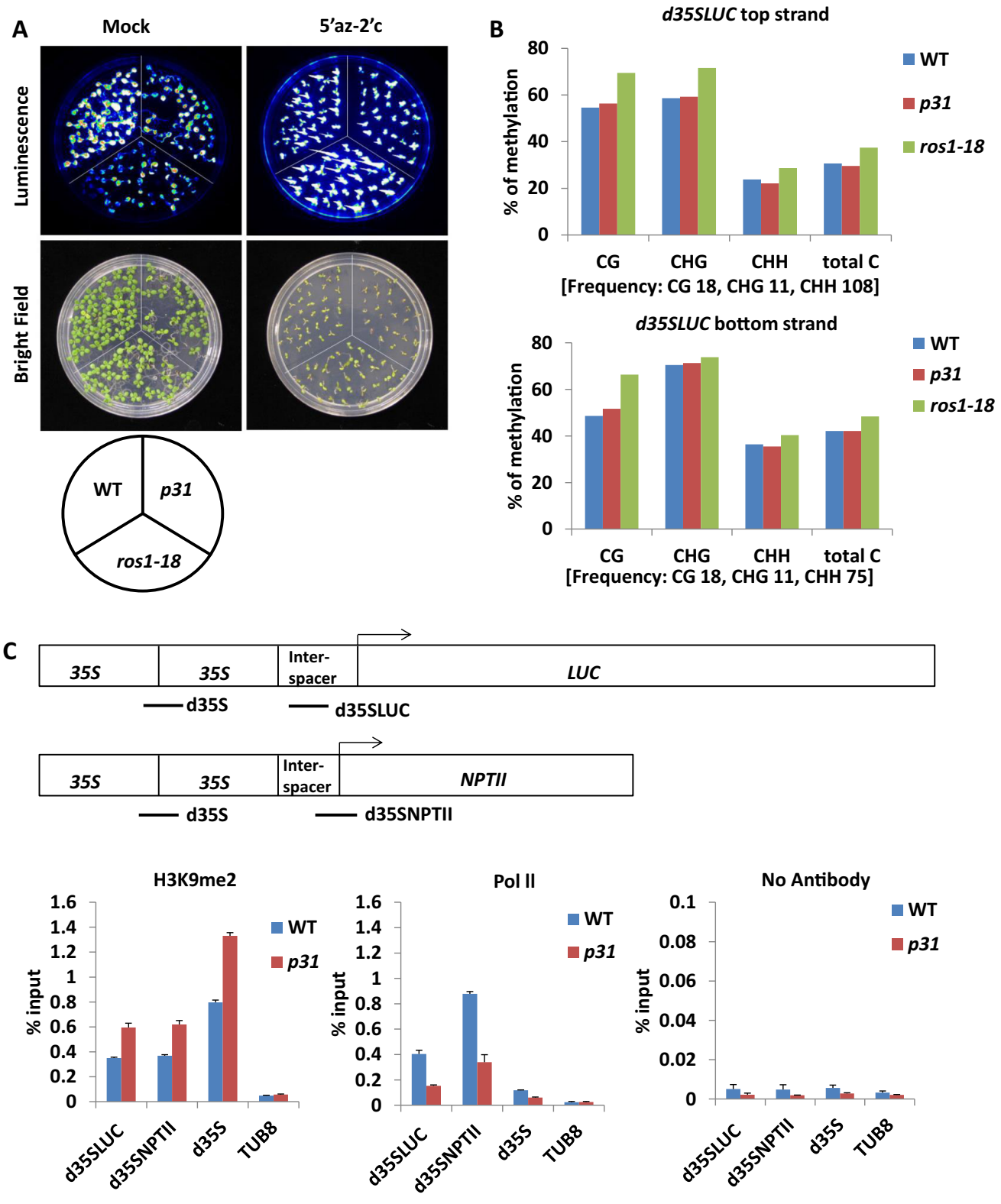

Figure 2. Epigenetic regulation and transcriptional silencing of *d35S::LUC* in the *p31* mutant. (**A**) Effect of 5-aza-2-deoxycytidine (5′az-2′c) on *d35S::LUC* expression in *p31* mutant plant. Seeds were sowed on $\frac{1}{2}$ MS with or without 7 μg/ml 5′az-2′c and grown for 10 days before imaged. (**B**) DNA methylation levels of the *d35S* promoter region as measured by bisulfite sequencing in the top and bottom strands. (**C**) ChIP-qPCR analyses of H3K9me2 levels and RNA polymerase Pol II occupancy at *d35S* promoter regions in the *p31* mutant compared to WT. The examined regions are shown in the schematic diagram. Errors bars indicate SD from three technical repeats. Results were confirmed by three biological replicates. Anti-H3K9me2 and anti-Pol II CTD repeat YSPTSPS were used. Promoter of *Tubulin 8* (*TUB8*) was used as a non-specific control region.

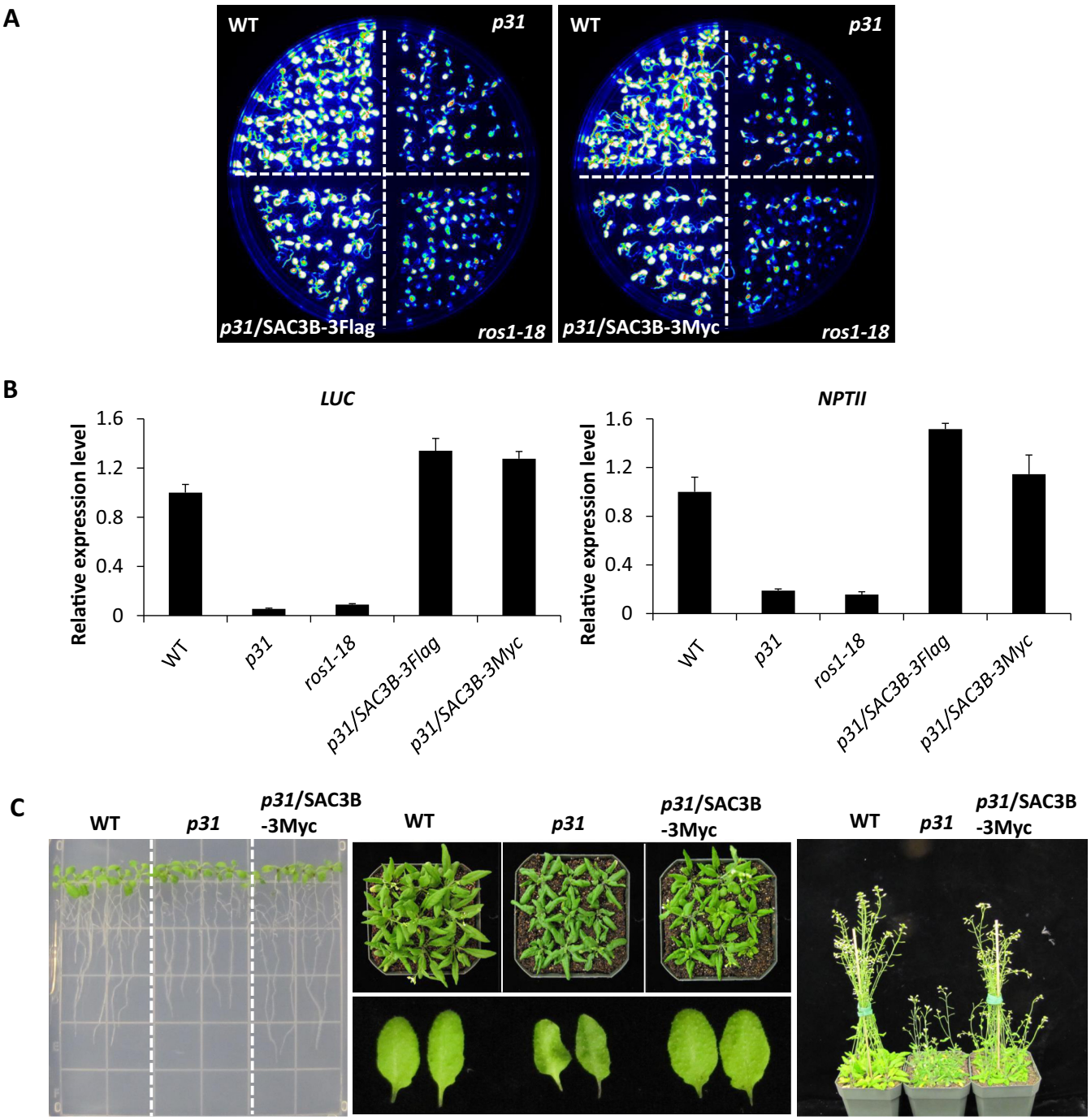

Figure 3. Complementation of SAC3B in the *p31* mutant restored transgene expression as determined by (**A**), luciferase luminescence signals and (**B**), quantitative real time PCR analyses. Two complementation lines with different epitope tags, *p31*/SAC3B-3Flag and *p31*/SAC3B-3Myc are shown. Error bars indicate SEM from three biological replicates. (**C**) Complementation of SAC3B rescued morphological phenotypes of *p31*.

metabolic processes, response to auxin and other hormonal stimuli, while the down-regulated genes are largely related to defense responses (Supplementary Figure S4A and B). These differential gene expression patterns, in combination with the morphological phenotypes caused by *sac3b* mutation, demonstrate important roles of SAC3B in growth and developmental processes, as well as indicate potential roles of SAC3B-mediated RNA export in defense, although regulation of some DEGs by RNA-export may be indirect. We examined characteristics of the DEGs in terms of gene length, GC content and transcript abundance (Supplementary Figure S4C). It appears that, compared to genome-wide average numbers, the up-regulated genes tend to have shorter gene length and lower expression levels, while down-regulated genes tend to have higher expression levels (Supplementary Figure S4C).

A

NUA and THP1 were co-immunoprecipitated with SAC3B-3XFlag

Gene	Protein	prot_score	prot_mass	Times detected (of 4 biological repeats)
At3g06290	SAC3B	5950	191523	4
At1g79280	NUA	312	237637	4
At2g19560	THP1	171	47983	4

B

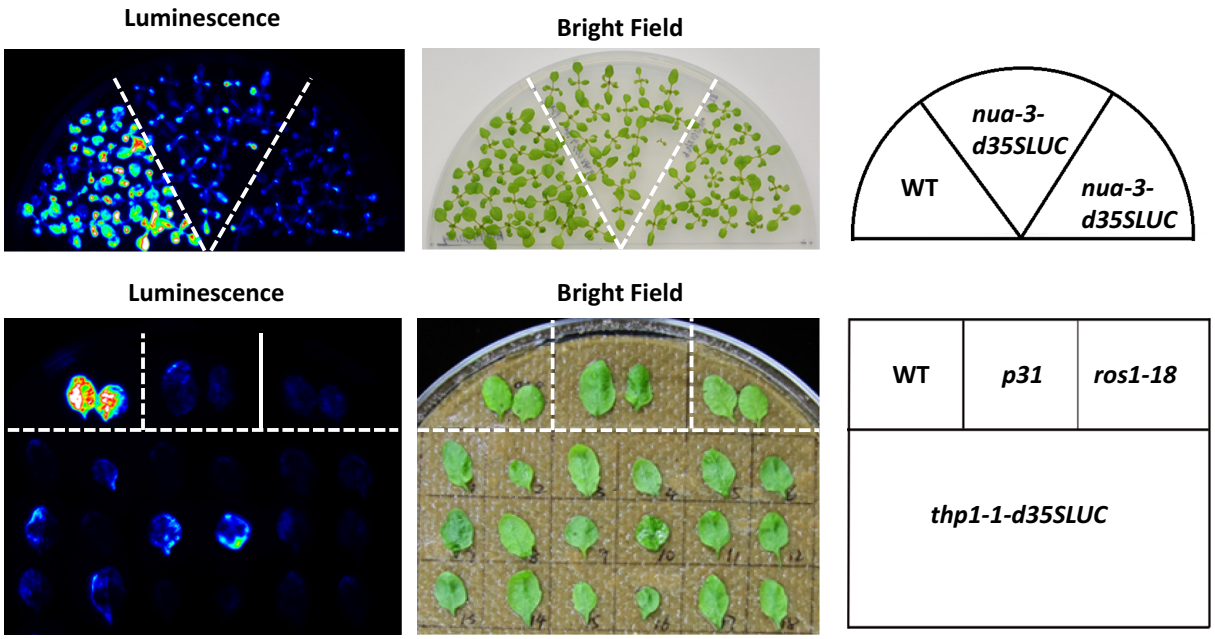

C

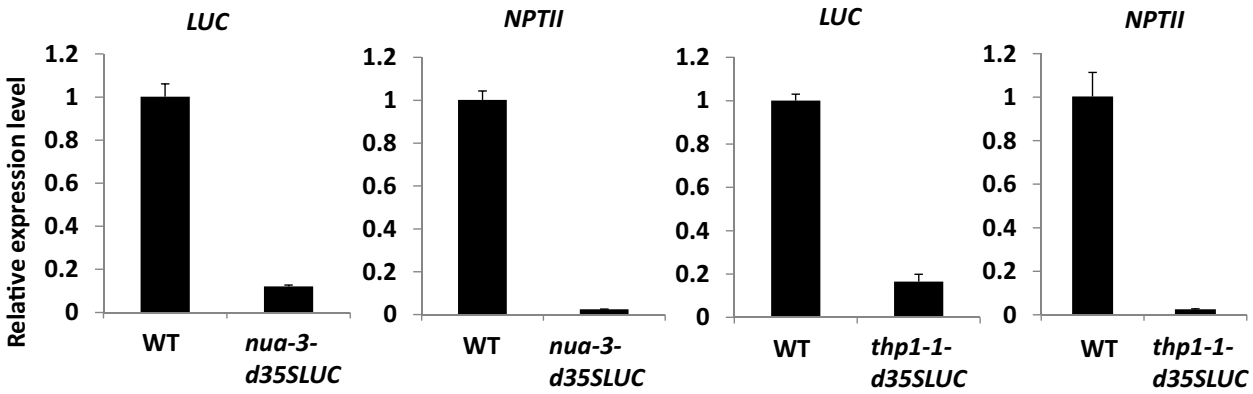

Figure 4. Mutations of SAC3B-associated NUA and THP1 also cause *d35S::LUC* gene silencing. (**A**) NUA and THP1 were identified as SAC3B-associated proteins by co-immunoprecipitation followed by mass spectrometry analysis (IP-MS). (**B**) Mutation of NUA or THP1 causes *d35S::LUC* gene silencing as indicated by decreased luminescence signals. (**C**) Mutation of NUA or THP1 causes *d35S::LUC* gene silencing as measured by RT-qPCR. Error bars indicate SEM from three biological repeats.

Beta-amylase 5 (At4g15210) is one of the DEGs with a drastically repressed expression in the absence of SAC3B. Similar to the *d35S::LUC* transgene, beta-amylase 5 also displays heavy DNA methylation in gene promoter region (Supplementary Figure S5E). We thus compared the gene-silencing patterns at these two loci. As shown in Supplementary Figure S5A, At4g15210 transcript level is decreased in both *p31* and *sac3b-7* mutants compared to their corresponding controls, confirming that the gene silencing is caused by *sac3b* mutation (Supplementary Figure S5A and B). As a result of SAC3B dysfunction, H3K9 dimethylation level is increased at the At4g15210 promoter region, while Pol II occupancy is decreased (Supplementary Figure S5C and D). Similar patterns of transcriptional gene regulation were also observed at At3g28550 and At2g05510 (Supplementary Figure S5), which also displayed gene reduction in *sac3b* mutants. Therefore, SAC3B functions as an anti-silencing factor that permits proper transcription activities at both transgenic and endogenous loci.

Gene silencing in *sac3b* mutants is independent of R-loop accumulation

In yeast and animal cells, mutations of RNA export factors can cause the accumulation of RNA–DNA hybrid (R-loop) that results in disruption of Pol II transcription and inducing heterochromatin formation (49–51). We thus questioned whether *sac3b* mutation causes R-loop accumulation that leads to disruption of Pol II transcription and thereby gene silencing. In *Arabidopsis*, R-loop was detected at the *FLC* locus, where both sense and anti-sense transcripts are negatively affected by R-loop accumulation (36). Our mRNAseq data showed a lower *FLC* expression level in *sac3b-7* compared to Col-0 (Figure 5A). Quantitative real time PCR results confirmed *FLC* expression reduction in both *sac3b-7* and *p31* (Figure 5B). However, expression levels of the *FLC* anti-sense transcript, *COOLAIR*, were not affected by *sac3b* mutations (Figure 5C). Although FLC is known as a negative regulator of flowering time control, we did not observe early flowering in *sac3b* mutants (data not shown). In fact, expression of several key factors downstream of FLC in controlling flowering time, including *FT*, *SOC1* and *AP1*, was not increased as a result of *FLC* down-regulation from our mRNAseq data (data not shown). This indicates that FLC is not the sole regulator of its downstream factors, at least under our experimental conditions.

We next performed DNA IP experiments to examine R-loop formation by using the S9.6 antibody that specifically recognizes RNA–DNA hybrid (52). RNA–DNA hybrid was detected as expected at the promoter region of *COOLAIR* in both WT and *p31* (Figure 5E). Previous study has showed high and very low R-loop signals at the *FLC*-h and *FLC*-e subregions, respectively (36). We also observed higher levels of R-loop at the *FLC*-h subregion than *FLC*-e, consistent with the previous report (36). Importantly, the *p31* mutant displayed similar R-loop signals as those in WT (Figure 5E) at either *FLC*-h or *FLC*-e subregions. Therefore, *sac3b* mutation does not induce R-loop accumulation, at least not at the *COOLAIR* promoter region.

We subsequently examined *d35S::LUC* for possible R-loop accumulation. As shown in Figure 5D, three subregions (namely I, II and III) of the *d35S::LUC* promoter were examined. The existence of R-loop at *d35S::LUC* promoter region was exhibited by the higher signal levels in samples without RNase H treatment compared to those treated with RNase H (Figure 5E), which specifically cleaves RNA in RNA–DNA hybrid. At all examined subregions, *p31* displayed similar levels of R-loop signals as those in WT (Figure 5E), therefore excluding the possibility that *sac3b* mutation causes transcriptional silencing through R-loop accumulation.

In addition to DNA IP using S9.6 antibody, we also performed R-loop footprinting experiment, in which cytosine (C) at the non-protected single strand can be converted into uracil (U) by a native sodium bisulfite treatment, and the mutation profile of the ssDNA allows definition of the R-loop position (36). Similar to the previous report (36), we detected C to T conversion events at the *FLC* locus (Supplementary Figure S6A). Our results showed RNA–DNA hybrid near the junction of the 2nd 35S sequence and the interspacer sequence, ranging from 30 bp to 300 bp (Supplementary Figure S6B and C). Specifically, C to T conversion was detected in the coding strand of *d35S::LUC* sequence but not in the template strand (Supplementary Figure S6B, S6C and S7), indicating that the coding strand is the single strand in the R-loop structure, while the template strand forms RNA–DNA hybrid together with sense *d35S::LUC* transcript. Together, our results revealed that, despite of the existence of R-loop at the *d35S::LUC* promoter, gene silencing in *sac3b* mutants is independent of R-loop accumulation.

SAC3B mutations alter small RNAs accumulation

Given that some siRNAs, such as trans-acting siRNAs (tasiRNAs), are derived from precursor RNAs that are subject to processing by RDR6 and SGS3 in the cytoplasm (27,53,54), we carried out genome-wide investigation on the potential involvement of SAC3B in regulating siRNA biogenesis. Whole-genome small RNA deep sequencing was performed by using two *sac3b* T-DNA insertion lines, *sac3b-7* and *sac3b-3*. Our analyses revealed similar patterns of small RNA size (18–32 nt) distribution as well as global small RNA abundance (Supplementary Figure S8A), indicating that SAC3B is not a major regulator in small RNA biogenesis. Nevertheless, we identified 635 differential small RNA regions (DSRs) where levels of total small RNAs (18–32 nt) were decreased by ≥3-folds in both *sac3b-7* and *sac3b-3* compared to Col-0 (Figure 6A; Supplementary Figure S8B). In addition, we also identified 550 DSRs where total small RNAs were increased by ≥3-folds in both *sac3b* mutants (Figure 6A; Supplementary Figure S8C). Specifically, *sac3b-7* and *sac3b-3* commonly showed 407 and 405 DSRs where 24 nt siRNA levels were decreased and increased, respectively (Supplementary Figure S8B and C). As expected, the majority of all 24 nt siRNA DSRs fall into the category of transposons (Supplementary Figure S8B and C), which are known as hotspots of siRNA production (55). Meanwhile, *sac3b-7* and *sac3b-3* also shared 81 and 48 DSRs where 21 nt siRNA levels were decreased and increased, respectively (Supplementary Figure S8B and C).

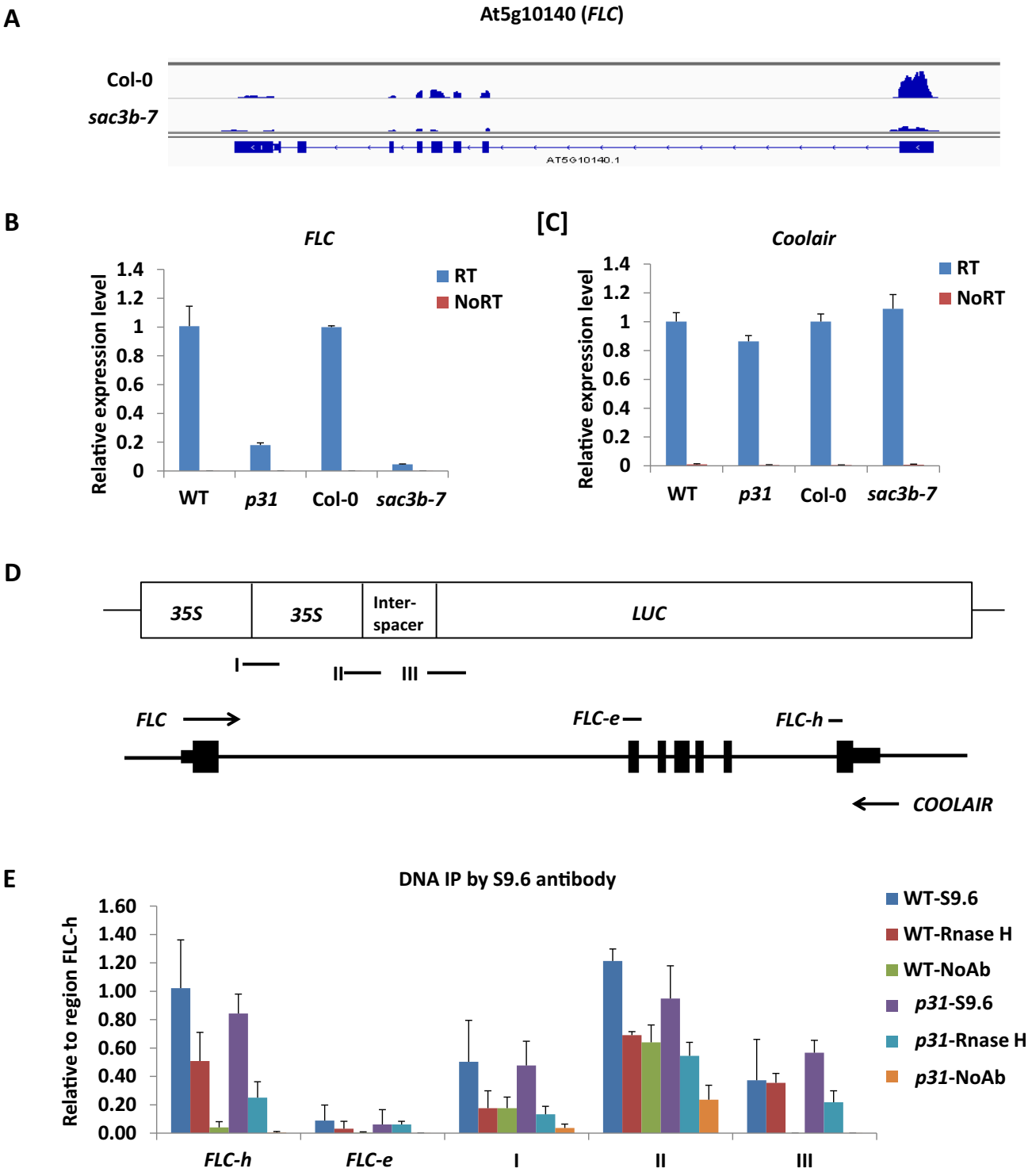

Figure 5. Gene silencing in *sac3b* mutants is independent of R-loop accumulation. (**A**) A snapshot of RNAseq data showing *FLC* expression is decreased in the *sac3b-7* mutant. (**B**) Reduced *FLC* gene expression in *p31* and *sac3b-7* mutants by RT-qPCR. (**C**) *COOLAIR* transcript levels in *sac3b* mutant alleles; RT-qPCR results are shown. Error bars are SEM, n = 3 biological replicates. (**D**) Schematic of *d35S::LUC* and *FLC* gene structure showing the examined subregions (I, II, III, *FLC-h*, *FLC-e*) in DNA IP assays. (**E**) R-loop detection by DNA IP followed by qPCR. The S9.6 antibody was used for DNA IP. Values of R-loop enrichment were divided by input and normalized to *FLC*-h region. Error bars indicate SD from three technical repeats. Results were confirmed by three biological replicates. R-loop signals were confirmed by RNase H treatment that specifically degrades RNA within DNA:RNA hybrid. NoAb: no antibody control.

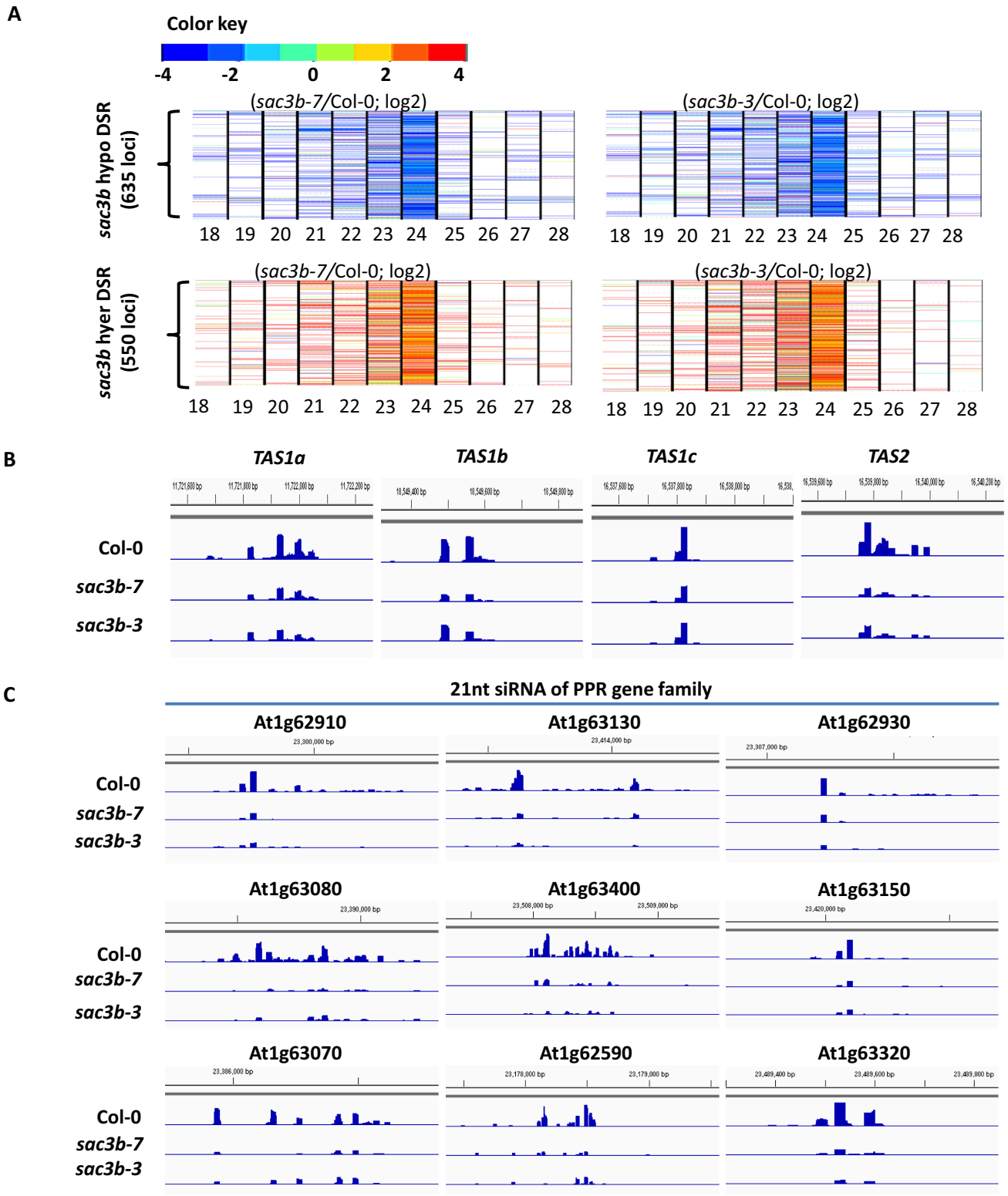

Figure 6. SAC3B mutation alters small RNA accumulation. (**A**) Heatmap depiction of the 635 hypo-DSR and the 550 hyper-DSR, where small RNA levels are decreased and increased, respectively, in both *sac3b-7* and *sac3b-3* mutants. (**B**) SAC3B dysfuntion reduces the levels of tasiRNA and 21 nt siRNA from a group of (**C**) TAS-like PRR gene loci. Snapshots from whole-genome small RNA sequencing are shown, with vertical blue bars indicating the siRNA sequencing coverage normalized to the same scale in the WT and mutants.

SAC3B dysfunction causes reduced abundance of tasiRNAs incuding *TAS1a*, *TAS1b*, *TAS1c* and *TAS2* (Figure 6B). In contrast to *TAS1* and *TAS2* tasiRNAs, *TAS3* tasiRNAs were unaffected by *sac3b* mutations (Supplementary Figure S9B). A previous study identified additional tasiRNA-like loci, which include nine genes encoding closely related PPR proteins (56). We checked these tasiRNA-like loci, and found that 21 nt siRNA abundance was decreased at all of these nine PPR genes in *sac3b* mutants (Figure 6C). In addition, the small RNA levels at the *IR71* locus were moderately decreased in *sac3b-7* and *sac3b-3* compared to Col-0 (Supplementary Figure S9B). Small RNA accumulation at *TAS1*, *TAS2* and *IR71* loci were previously shown to be decreased in Arabidopsis mutant defective in the TREX complex (27). Since the TREX and TREX-2 complexes both regulate RNA nucleo-cytoplasmic export, it appears that the dependence of these small RNAs on the TREX-2 complex is mediated through RNA export.

SAC3B has a clear albeit minor effect on DNA methylome

Because *sac3b* mutations disrupt siRNA accumulation at hundreds of loci, we performed whole-genome bisulfite sequencing to explore potential involvement of SAC3B in DNA methylation, since in Arabidopsis DNA methylation can be mediated through siRNAs. Totally 537 and 467 DNA hypo-methylation loci were identified in *sac3b-7* and *sac3b-3*, respectively (Supplementary Figure S10). On the other hand, 575 and 447 DNA hyper-methylation loci were identified in *sac3b-7* and *sac3b-3*, respectively (Supplementary Figure S10). Among these DMRs, 200 hypo-DMRs and 121 hyper-DMRs are shared by the two *sac3b* mutant alleles (Supplementary Figure S10), therefore demonstrating a clear albeit minor contribution of SAC3B in shaping the Arabidopsis DNA methylome.

RdDM in plants involves 24 nt siRNA that are dependent on the plant-specific RNA polymerase Pol IV. Reduction in 24 nt siRNA levels was observed at the 200 hypo-DMRs shared by *sac3b-7* and *sac3b-3* (Figure 7A), indicating that these SAC3B-dependent hypo-DMRs are targets of canonical RdDM pathway. Indeed, at the 200 SAC3B-dependent DMRs, cytosine methylation was similarly reduced in *sac3b* mutants as well as in *nrpd1a-3* and *nrpd1b-11*, which are two RdDM mutants defective in Pol IV and Pol V, respectively (Figure 7B). For instance, the Chr1:20462501-20463000 and Chr5:3715001-3715100 loci are targeted by RdDM, while functional SAC3B is required for proper accumulation of 24 nt siRNA and DNA methylation at these loci (Figure 7C). In addition to 24 nt siRNA, certain 21 nt siRNA such as tasiRNA can also be correlated to DNA methylation in Arabidopsis (57). In the *sac3b* mutants, decreased DNA methylation levels were observed at loci of *TAS1a*, *TAS1b*, *TAS1c* and *TAS2* (Figure 7D; Supplementary Figure S9A), concurrent with the reduced levels of tasiRNAs. However, DNA methylation seemed unchanged at the *IR71* locus (Supplementary Figure S9B), where DNA methylation is mediated by 24 nt siRNA (55). Since SAC3B dysfunction reduces but does not abolish 24 nt siRNA levels at *IR71*, it is possible that the remaining 24 nt siRNA level is still sufficient to mediate DNA methylation at this locus. Thus, concurrent reduction in siRNA and DNA methylation levels in both *sac3b-7* and *sac3b-3* mutant alleles supports a role of SAC3B in epigenetic regulation.

DISCUSSION

In this study, we identified SAC3B as an anti-silencing factor that regulates transgenic reporter and endogenous genes in Arabidopsis. The same genetic screen also recovered a *ros1* mutant allele, in which transcriptional silencing can be attributed to DNA hypermethylation that results from a loss of the DNA demethylase ROS1. While SAC3B and ROS1 are both required to protect *d35S::LUC* from being silenced, the two anti-silencing factors clearly displayed different mechanisms, because DNA methylation at *d35S::LUC* promoter is increased in *ros1* but is unaffected by *sac3b* mutation. Therefore, these results highlight the co-regulation of gene transcription by two different mechanisms.

SAC3 proteins are conserved in eukaryotes as a core component of the TREX-2 complex. In yeast, mutations of the TREX-2 complex can cause R-loop accumulation which inhibits Pol II transcription (25); while other studies found that R-loops are linked to chromatin condensation and heterochromatin formation (50,51). In our study, R-loop was detected at the silenced gene loci in *sac3b* mutant as well as in the WT plants, however, *sac3b* mutation does not affect R-loop accumulation levels, indicating that the mechanism of SAC3-mediated anti-silencing in plants can be different from that in yeast.

Despite the possibility that defects in mRNA export may lead to abnormal accumulation and consequently degradation of RNAs in the nucleus, the observations of decreased Pol II occupancy and increased H3K9me2 levels in *sac3b* and *nua* mutants demonstrated that the gene silencing events, at least in part, occur at transcriptional level and involve epigenetic modifications. At the examined loci, the *sac3b* mutant displayed higher levels of H3K9me2 than WT, indicating that SAC3B prevents formation of heterochromatin at the transcribed loci. IP-MS analyses revealed physical association of SAC3B and the nuclear pore complex protein NUA, while mutation of NUA causes gene silencing of *d35S::LUC* as well. Similarly, SAC3B interacts with another TREX-2 component, THP1, whose mutation also causes suppression of *d35S::LUC* gene expression. These results brought up a possibility that the TREX-2 complex anchors its target genes, such as *d35S::LUC*, to the NPC and thereby creates decondensed chromatin regions to facilitate Pol II transcription, in consistence with the 'gene gating' hypothesis.

The 'gene gating' hypothesis envisions that certain decondensed chromatin regions containing transcribable genes are attached to the NPC (58). Supporting this hypothesis, several highly induced genes in yeast are randomly distributed in the nucleoplasm when transcriptionally repressed but are recruited to the nuclear periphery upon activation (59–61). For instance, the *GAL1*, *GAL2*, *GAL7* and *GAL10* genes were greatly induced in response to galactose. Upon glactose induction, the *GAL* genes relocalize to the nuclear periphery and associate with the nucleoporin proteins (61,62). Similarly, the *INO1* gene localizes throughout the nucleoplasm when repressed, but is recruited to the nu-

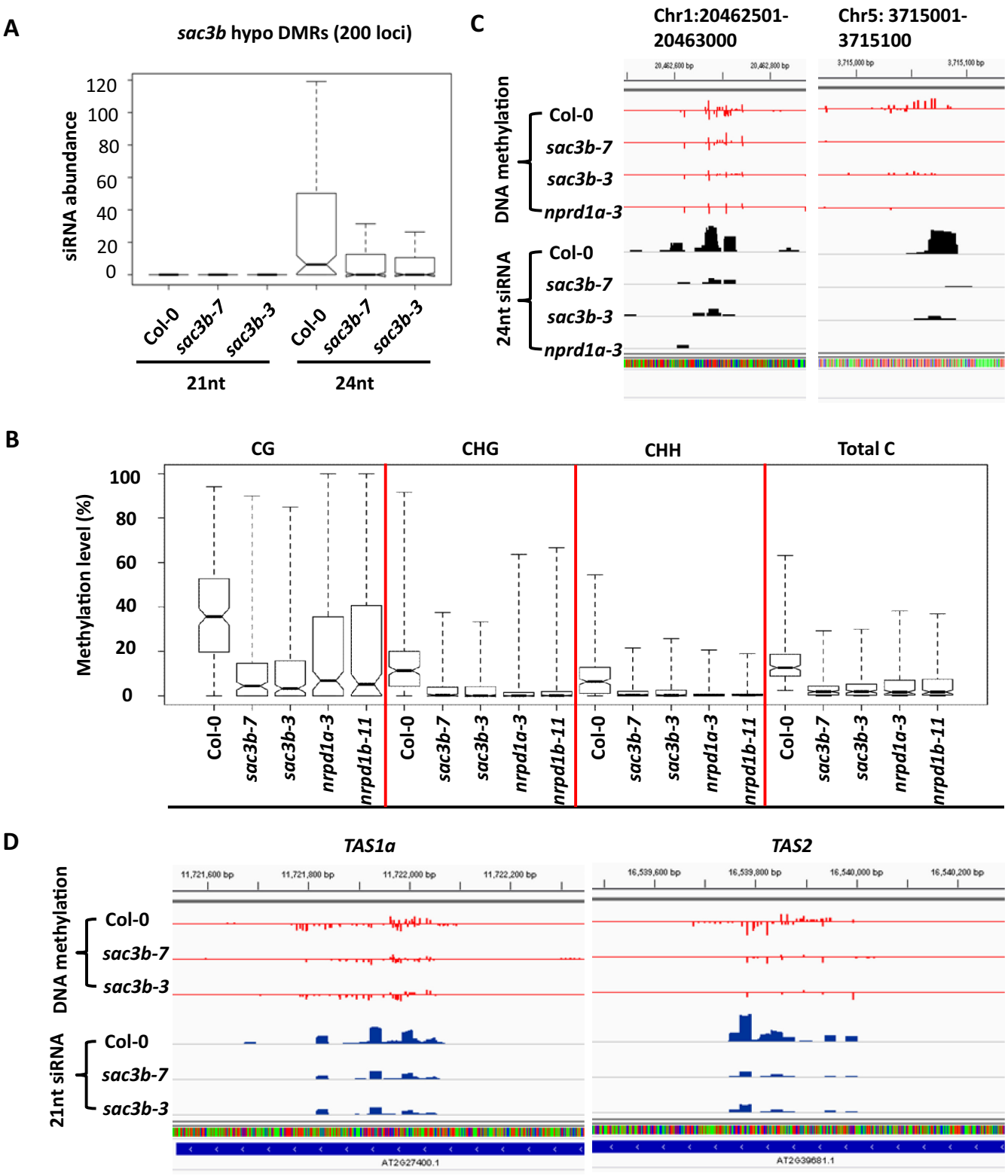

Figure 7. SAC3B mutation disrupts RNA-directed DNA methylation at a number of loci. (**A**) A box plot showing comparison of siRNA abundance between WT and *sac3b* mutants at the 200 SAC3B-dependent hypo-DMRs. (**B**) Box-plots showing DNA methylation level of *sac3b* mutants, *nrpd1a-3* and *nrpd1b-11* at the 200 SAC3B-dependent hypo-DMRs. (**C**) Two examples of RdDM loci where levels of DNA methylation and 24 nt siRNA require functional SAC3B. Snapshots from whole-genome bisulfite sequencing and whole-genome small RNA sequencing were shown. (**D**) SAC3B mutations decrease the levels of 21 nt tasiRNA and of local DNA methylation. See also Supplementary Figure S9A.

clear periphery upon transcriptional activation; meanwhile artificial recruitment of *INO1* gene to the nuclear membrane permits activation (60). Further experiments found that most nucleoporins and karyopherins preferentially associate with a subset of highly transcribed genes (61). These findings indicate that the NPC tethering correlates with gene transcriptional activity. Indeed, a recent study in yeast found that TREX-2 complex interact with the Mediator complex, an essential regulator of Pol II and that Mediator and TREX-2 are both required for NPC targeting of the highly inducible *GAL1* and *HXK1* genes (63). In our study, the reporter gene luciferase is under control of double *35S* promoter, which is a well-known strong promoter; while At4g15210 expression is highly inducible by sucrose (64). Thus, it is possible that these genes are targeted to NPC through the TREX-2 complex, which not only couples transcription with mRNA export but also facilitates chromatin decondensation and Pol II transcription.

Proteins that function in nuclear transport may also play a role in epigenetic regulation (65). In budding yeast it was found that various proteins involved in nuclear transport harbor robust chromatin boundary activity that blocks propagation of heterochromatin by direct or indirect tethering of the cis-acting elements to the Nup2p receptor of the nuclear pore complex (65). Moreover, nuclear transport proteins can also mediate epigenetic transcriptional memory (66). For example, the *INO1* gene is transcriptionally repressed upon shifting from activating to repressing condition, but it remains primed for reactivation at the nuclear periphery for several generations. Transcriptional memory of *INO1* is lost in cells lacking the NPC protein Nup100, resulting in nucleoplasmic localization and slower reactivation of the gene (67). Thus, interaction of specific gene sequence with the NPC may alter its epigenetic status. The promoter of *d35S::LUC* transgene is under control of epigenetic marks (29; this study). Importantly, our results showed that, in the absence of SAC3B, the level of heterochromatin mark H3K9me2 was increased at the the *d35S* promoter region of the reporter gene, whereas SAC3B mediates the association between TREX-2 and NUA. Thus, it is possible that the TREX-2 complex bridges the *d35S::LUC* transgene with the nuclear pore complex, thereby placing the transgene in an epigenetic environment that is favorable for transcription.

In addition to regulating mRNA transcription, SAC3B is also involved in biogenesis of a number of small RNAs. Mutation of SAC3B decreases the levels of most tasiRNAs as well as siRNAs that originated from a group of *TAS*-like loci. Such an observation is consistent with the function of SAC3B in mediating RNA nucleo-cytoplasmic transport, because tasiRNAs are derived from their corresponding precursor RNAs that need cooperative processing by RDR6 and SGS3 in the cytoplasm (53,68). Similar to the TREX-2 complex, a functional TREX complex was shown be required for accumulation of several tasiRNAs (27). In our study, the role of RNA-export on small RNA production was examined by genome-wide profiling, which also highlight specific regulation by SAC3B on *TAS* and *TAS*-like loci.

Although *sac3b* mutation does not affect DNA methylation levels at the *d35S::LUC* promoter, whole-genome bisulfite sequencing revealed a few hundred of genomic loci where alterations in DNA methylation levels were commonly observed in the two examined alleles of *sac3b* mutants. In contrast to the limited numbers of DMRs in *sac3b* mutants, thousands of hyper- and hypo-DMRs have been identified in the well-known epigenetic mutants including *ros1-4* and *nrpd1a-3,* which are defective in the DNA demethylase ROS1 and a key RdDM component Pol IV, respectively (39,69). Therefore, SAC3B-mediated regulation represents a minor albeit clear contribution to the DNA methylome in Arabidopsis. The histone mark H3K9me2 facilitates recruitment of Pol IV, which is responsible for 24 nt siRNA production, to loci that are targets of RNA-directed DNA methylation (70), whereas SAC3B prevents silencing of Pol II transcription in a way that is correlated with decreased H3K9me2 levels (Figure 2C). Meanwhile abundance of 24 nt siRNA was reduced at regions where DNA methylation was decreased by *sac3b* mutation. Thus, it appears that SAC3B mediation of siRNA production at these loci is unrelated to SAC3B regulation of H3K9me2. It remains unclear whether production of 24 nt siRNAs at these SAC3B-dependent loci requires nucleo-cytoplasmic transport of precursor RNAs.

SUPPLEMENTARY DATA

Supplementary Data are available at NAR Online.

ACKNOWLEDGEMENT

The authors thank Dr Xuemei Chen (Department of Botany and Plant Sciences, University of California, Riverside) for kindly providing the YJ report line.

FUNDING

Chinese Academy of Sciences [CAS Pioneer Hundred TalentsProgram to H.Z.]; Chinese Academy of Sciences and the US National Institutes of Health Grants [to J.-K.Z.]; China Scholarship Council [to Y.Y.]. Funding for open access charge: CAS Pioneer Hundred Talents Program [to H. Z.].
Conflict of interest statement. None declared.

REFERENCES

1. Slotkin,R.K. and Martienssen,R. (2007) Transposable elements and the epigenetic regulation of the genome. *Nat. Rev. Genet.*, **8**, 272–285.
2. Holoch,D. and Moazed,D. (2015) RNA-mediated epigenetic regulation of gene expression. *Nat. Rev. Genet.*, **16**, 71–84.
3. Matzke,M.A. and Mosher,R.A. (2014) RNA-directed DNA methylation: an epigenetic pathway of increasing complexity. *Nat. Rev. Genet.*, **15**, 394–408.
4. Law,J.A. and Jacobsen,S.E. (2010) Establishing, maintaining and modifying DNA methylation patterns in plants and animals. *Nat. Rev. Genet.*, **11**, 204–220.
5. Zemach,A., Kim,M.Y., Hsieh,P.H., Coleman-Derr,D., Eshed-Williams,L., Thao,K., Harmer,S.L. and Zilberman,D. (2013) The Arabidopsis nucleosome remodeler DDM1 allows DNA methyltransferases to access H1-containing heterochromatin. *Cell*, **153**, 193–205.
6. Cao,X. and Jacobsen,S.E. (2002) Role of the arabidopsis DRM methyltransferases in de novo DNA methylation and gene silencing. *Curr. Biol.*, **12**, 1138–1144.

7. Liu,C.Y., Lu,F.L., Cui,X. and Cao,X.F. (2010) Histone Methylation in Higher Plants. *Annu. Rev. Plant Biol.*, **61**, 395–420.
8. Rea,S., Eisenhaber,F., O'Carroll,D., Strahl,B.D., Sun,Z.W., Schmid,M., Opravil,S., Mechtler,K., Ponting,C.P., Allis,C.D. *et al.* (2000) Regulation of chromatin structure by site-specific histone H3 methyltransferases. *Nature*, **406**, 593–599.
9. Henderson,I.R. and Jacobsen,S.E. (2008) Tandem repeats upstream of the Arabidopsis endogene SDC recruit non-CG DNA methylation and initiate siRNA spreading. *Genes Dev.*, **22**, 1597–1606.
10. Soppe,W.J., Jacobsen,S.E., Alonso-Blanco,C., Jackson,J.P., Kakutani,T., Koornneef,M. and Peeters,A.J. (2000) The late flowering phenotype of fwa mutants is caused by gain-of-function epigenetic alleles of a homeodomain gene. *Mol. Cell*, **6**, 791–802.
11. Zhu,J.K. (2009) Active DNA demethylation mediated by DNA glycosylases. *Annu. Rev. Genet.*, **43**, 143–166.
12. Gong,Z., Morales-Ruiz,T., Ariza,R.R., Roldan-Arjona,T., David,L. and Zhu,J.K. (2002) ROS1, a repressor of transcriptional gene silencing in Arabidopsis, encodes a DNA glycosylase/lyase. *Cell*, **111**, 803–814.
13. Mittelsten Scheid,O., Probst,A.V., Afsar,K. and Paszkowski,J. (2002) Two regulatory levels of transcriptional gene silencing in Arabidopsis. *Proc. Natl. Acad. Sci. U.S.A.*, **99**, 13659–13662.
14. Wang,X., Duan,C.G., Tang,K., Wang,B., Zhang,H., Lei,M., Lu,K., Mangrauthia,S.K., Wang,P., Zhu,G. *et al.* (2013) RNA-binding protein regulates plant DNA methylation by controlling mRNA processing at the intronic heterochromatin-containing gene IBM1. *Proc. Natl. Acad. Sci. U.S.A.*, **110**, 15467–15472.
15. Lang,Z.B., Lei,M.G., Wang,X.G., Tang,K., Miki,D., Zhang,H.M., Mangrauthia,S.K., Liu,W.S., Nie,W.F., Ma,G.J. *et al.* (2015) The methyl-CpG-binding protein MBD7 facilitates active DNA demethylation to limit DNA hyper-methylation and transcriptional gene silencing. *Mol. Cell*, **57**, 971–983.
16. Perales,R. and Bentley,D. (2009) 'Cotranscriptionality': The transcription elongation complex as a nexus for nuclear transactions. *Mol. Cell*, **36**, 178–191.
17. Kohler,A. and Hurt,E. (2007) Exporting RNA from the nucleus to the cytoplasm. *Nat. Rev. Mol. Cell Biol.*, **8**, 761–773.
18. Strasser,K., Masuda,S., Mason,P., Pfannstiel,J., Oppizzi,M., Rodriguez-Navarro,S., Rondon,A.G., Aguilera,A., Struhl,K., Reed,R. *et al.* (2002) TREX is a conserved complex coupling transcription with messenger RNA export. *Nature*, **417**, 304–308.
19. Zenklusen,D., Vinciguerra,P., Wyss,J.C. and Stutz,F. (2002) Stable mRNP formation and export require cotranscriptional recruitment of the mRNA export factors Yra1p and Sub2p by Hpr1p. *Mol. Cell. Biol.*, **22**, 8241–8253.
20. Wente,S.R. and Rout,M.P. (2010) The nuclear pore complex and nuclear transport. *Cold Spring Harb. Perspect. Biol.*, **2**, a000562.
21. Fischer,T., Strasser,K., Racz,A., Rodriguez-Navarro,S., Oppizzi,M., Ihrig,P., Lechner,J. and Hurt,E. (2002) The mRNA export machinery requires the novel Sac3p-Thp1p complex to dock at the nucleoplasmic entrance of the nuclear pores. *EMBO J.*, **21**, 5843–5852.
22. Fischer,T., Rodriguez-Navarro,S., Pereira,G., Racz,A., Schiebel,E. and Hurt,E. (2004) Yeast centrin Cdc31 is linked to the nuclear mRNA export machinery. *Nat. Cell Biol.*, **6**, U840–U844.
23. Rodriguez-Navarro,S., Fischer,T., Luo,M.J., Antunez,O., Brettschneider,S., Lechner,J., Perez-Ortin,J.E., Reed,R. and Hurt,E. (2004) Sus1, a functional component of the SAGA histone acetylase complex and the nuclear pore-associated mRNA export machinery. *Cell*, **116**, 75–86.
24. Faza,M.B., Kemmler,S., Jimeno,S., Gonzalez-Aguilera,C., Aguilera,A., Hurt,E. and Panse,V.G. (2009) Sem1 is a functional component of the nuclear pore complex-associated messenger RNA export machinery. *J. Cell Biol.*, **184**, 833–846.
25. Gonzalez-Aguilera,C., Tous,C., Gomez-Gonzalez,B., Huertas,P., Luna,R. and Aguilera,A. (2008) The THP1-SAC3-SUS1-CDC31 complex works in transcription elongation-mRNA export preventing RNA-mediated genome instability. *Mol. Biol. Cell*, **19**, 4310–4318.
26. Tous,C. and Aguilera,A. (2007) Impairment of transcription elongation by R-loops in vitro. *Biochem. Biophys. Res. Commun.*, **360**, 428–432.
27. Yelina,N.E., Smith,L.M., Jones,A.M., Patel,K., Kelly,K.A. and Baulcombe,D.C. (2010) Putative Arabidopsis THO/TREX mRNA export complex is involved in transgene and endogenous siRNA biosynthesis. *Proc. Natl. Acad. Sci. U.S.A.*, **107**, 13948–13953.
28. Xu,C., Zhou,X. and Wen,C.K. (2015) HYPER RECOMBINATION1 of the THO/TREX complex plays a role in controlling transcription of the REVERSION-TO-ETHYLENE SENSITIVITY1 gene in Arabidopsis. *PLoS Genet.*, **11**, e1004956.
29. Lu,Q., Tang,X., Tian,G., Wang,F., Liu,K., Nguyen,V., Kohalmi,S.E., Keller,W.A., Tsang,E.W., Harada,J.J. *et al.* (2010) Arabidopsis homolog of the yeast TREX-2 mRNA export complex: components and anchoring nucleoporin. *Plant J.*, **61**, 259–270.
30. Wilmes,G.M. and Guthrie,C. (2009) Getting to the gate: crystallization of a Sac3(CID):Sus1:Cdc31 complex. *Mol. Cell*, **33**, 671–672.
31. Li,S., Liu,L., Gao,L., Zhao,Y., Kim,Y.J. and Chen,X. (2016) SUVH1, a Su(var)3-9 family member, promotes the expression of genes targeted by DNA methylation. *Nucleic Acids Res.*, **44**, 608–620.
32. Liu,F., Marquardt,S., Lister,C., Swiezewski,S. and Dean,C. (2010) Targeted 3′ processing of antisense transcripts triggers Arabidopsis FLC chromatin silencing. *Science*, **327**, 94–97.
33. Lei,M.G., Zhang,H.M., Julian,R., Tang,K., Xie,S.J. and Zhu,J.K. (2015) Regulatory link between DNA methylation and active demethylation in Arabidopsis. *Proc. Natl. Acad. Sci. U.S.A.*, **112**, 3553–3557.
34. Hetzl,J., Foerster,A.M., Raidl,G. and Mittelsten Scheid,O. (2007) CyMATE: a new tool for methylation analysis of plant genomic DNA after bisulphite sequencing. *Plant J.*, **51**, 526–536.
35. Saleh,A., Alvarez-Venegas,R. and Avramova,Z. (2008) An efficient chromatin immunoprecipitation (ChIP) protocol for studying histone modifications in Arabidopsis plants. *Nat. Protoc.*, **3**, 1018–1025.
36. Sun,Q.W., Csorba,T., Skourti-Stathaki,K., Proudfoot,N.J. and Dean,C. (2013) R-Loop Stabilization Represses Antisense Transcription at the Arabidopsis FLC Locus. *Science*, **340**, 619–621.
37. Gruntman,E., Qi,Y.J., Slotkin,R.K., Roeder,T., Martienssen,R.A. and Sachidanandam,R. (2008) Kismeth: Analyzer of plant methylation states through bisulfite sequencing. *BMC Bioinformatics*, **9**, 371
38. Law,J.A., Ausin,I., Johnson,L.M., Vashisht,A.A., Zhu,J.K., Wohlschlegel,J.A. and Jacobsen,S.E. (2010) A protein complex required for polymerase V transcripts and RNA-directed DNA methylation in arabidopsis. *Curr. Biol.*, **20**, 951–956.
39. Zhang,H., Ma,Z.Y., Zeng,L., Tanaka,K., Zhang,C.J., Ma,J., Bai,G., Wang,P., Zhang,S.W., Liu,Z.W. *et al.* (2013) DTF1 is a core component of RNA-directed DNA methylation and may assist in the recruitment of Pol IV. *Proc. Natl. Acad. Sci. U.S.A.*, **110**, 8290–8295.
40. Harris,E.Y., Ponts,N., Le Roch,K.G. and Lonardi,S. (2012) BRAT-BW: efficient and accurate mapping of bisulfite-treated reads. *Bioinformatics*, **28**, 1795–1796.
41. Duan,C.G., Zhang,H., Tang,K., Zhu,X., Qian,W., Hou,Y.J., Wang,B., Lang,Z., Zhao,Y., Wang,X. *et al.* (2015) Specific but interdependent functions for Arabidopsis AGO4 and AGO6 in RNA-directed DNA methylation. *EMBO J.*, **34**, 581–592.
42. Kim,D., Pertea,G., Trapnell,C., Pimentel,H., Kelley,R. and Salzberg,S.L. (2013) TopHat2: accurate alignment of transcriptomes in the presence of insertions, deletions and gene fusions. *Genome Biol.*, **14**, R36.
43. Anders,S., Pyl,P.T. and Huber,W. (2015) HTSeq–a Python framework to work with high-throughput sequencing data. *Bioinformatics*, **31**, 166–169.
44. Robinson,M.D., McCarthy,D.J. and Smyth,G.K. (2010) edgeR: a Bioconductor package for differential expression analysis of digital gene expression data. *Bioinformatics*, **26**, 139–140.
45. Du,Z., Zhou,X., Ling,Y., Zhang,Z. and Su,Z. (2010) agriGO: a GO analysis toolkit for the agricultural community. *Nucleic Acids Res.*, **38**, W64–W70.
46. Langmead,B., Trapnell,C., Pop,M. and Salzberg,S.L. (2009) Ultrafast and memory-efficient alignment of short DNA sequences to the human genome. *Genome Biol.*, **10**, R25.
47. Peragine,A., Yoshikawa,M., Wu,G., Albrecht,H.L. and Poethig,R.S. (2004) SGS3 and SGS2/SDE1/RDR6 are required for juvenile development and the production of trans-acting siRNAs in Arabidopsis. *Genes Dev.*, **18**, 2368–2379.
48. Jacob,Y., Mongkolsiriwatana,C., Veley,K.M., Kim,S.Y. and Michaels,S.D. (2007) The nuclear pore protein AtTPR is required for RNA homeostasis, flowering time, and auxin signaling. *Plant Physiol.*, **144**, 1383–1390.

49. Huertas,P. and Aguilera,A. (2003) Cotranscriptionally formed DNA:RNA hybrids mediate transcription elongation impairment and transcription-associated recombination. *Mol. Cell*, **12**, 711–721.
50. Nakama,M., Kawakami,K., Kajitani,T., Urano,T. and Murakami,Y. (2012) DNA-RNA hybrid formation mediates RNAi-directed heterochromatin formation. *Genes Cells*, **17**, 218–233.
51. Castellano-Pozo,M., Santos-Pereira,J.M., Rondon,A.G., Barroso,S., Andujar,E., Perez-Alegre,M., Garcia-Muse,T. and Aguilera,A. (2013) R loops are linked to histone H3 S10 phosphorylation and chromatin condensation. *Mol. Cell*, **52**, 583–590.
52. Boguslawski,S.J., Smith,D.E., Michalak,M.A., Mickelson,K.E., Yehle,C.O., Patterson,W.L. and Carrico,R.J. (1986) Characterization of monoclonal-antibody to DNA. RNA and its application to immunodetection of hybrids. *J. Immunol. Methods*, **89**, 123–130.
53. Kumakura,N., Takeda,A., Fujioka,Y., Motose,H., Takano,R. and Watanabe,Y. (2009) SGS3 and RDR6 interact and colocalize in cytoplasmic SGS3/RDR6-bodies. *FEBS Lett.*, **583**, 1261–1266.
54. Jauvion,V., Elmayan,T. and Vaucheret,H. (2010) The conserved RNA trafficking proteins HPR1 and TEX1 are involved in the production of endogenous and exogenous small interfering RNA in Arabidopsis. *Plant Cell*, **22**, 2697–2709.
55. Zhang,X., Henderson,I.R., Lu,C., Green,P.J. and Jacobsen,S.E. (2007) Role of RNA polymerase IV in plant small RNA metabolism. *Proc. Natl. Acad. Sci. U.S.A.*, **104**, 4536–4541.
56. Howell,M.D., Fahlgren,N., Chapman,E.J., Cumbie,J.S., Sullivan,C.M., Givan,S.A., Kasschau,K.D. and Carrington,J.C. (2007) Genome-wide analysis of the RNA-DEPENDENT RNA POLYMERASE6/DICER-LIKE4 pathway in Arabidopsis reveals dependency on miRNA- and tasiRNA-directed targeting. *Plant Cell*, **19**, 926–942.
57. Wu,L., Mao,L. and Qi,Y. (2012) Roles of dicer-like and argonaute proteins in TAS-derived small interfering RNA-triggered DNA methylation. *Plant Physiol.*, **160**, 990–999.
58. Blobel,G. (1985) Gene gating: A hypothesis. *Proc. Natl. Acad. Sci. U.S.A.*, **82**, 8527–8529.
59. Taddei,A., Van Houwe,G., Hediger,F., Kalck,V., Cubizolles,F., Schober,H. and Gasser,S.M. (2006) Nuclear pore association confers optimal expression levels for an inducible yeast gene. *Nature*, **441**, 774–778.
60. Brickner,J.H. and Walter,P. (2004) Gene recruitment of the activated INO1 locus to the nuclear membrane. *PLoS Biol.*, **2**, e342.
61. Casolari,J.M., Brown,C.R., Komili,S., West,J., Hieronymus,H. and Silver,P.A. (2004) Genome-wide localization of the nuclear transport machinery couples transcriptional status and nuclear organization. *Cell*, **117**, 427–439.
62. Lashkari,D.A., DeRisi,J.L., McCusker,J.H., Namath,A.F., Gentile,C., Hwang,S.Y., Brown,P.O. and Davis,R.W. (1997) Yeast microarrays for genome wide parallel genetic and gene expression analysis. *Proc. Natl. Acad. Sci. U.S.A.*, **94**, 13057–13062.
63. Schneider,M., Hellerschmied,D., Schubert,T., Amlacher,S., Vinayachandran,V., Reja,R., Pugh,B.F., Clausen,T. and Kohler,A. (2015) The nuclear pore-associated TREX-2 complex employs mediator to regulate gene expression. *Cell*, **162**, 1016–1028.
64. Mita,S., Suzuki-Fujii,K. and Nakamura,K. (1995) Sugar-inducible expression of a gene for beta-amylase in Arabidopsis thaliana. *Plant Physiol.*, **107**, 895–904.
65. Ishii,K., Arib,G., Lin,C., Van Houwe,G. and Laemmli,U.K. (2002) Chromatin boundaries in budding yeast: The nuclear pore connection. *Cell*, **109**, 551–562.
66. Brickner,D.G., Cajigas,I., Fondufe-Mittendorf,Y., Ahmed,S., Lee,P.C., Widom,J. and Brickner,J.H. (2007) H2A.z-mediated localization of genes at the nuclear periphery confers epigenetic memory of previous transcriptional state. *PLoS Biol.*, **5**, 704–716.
67. Light,W.H., Brickner,D.G., Brand,V.R. and Brickner,J.H. (2010) Interaction of a DNA zip code with the nuclear pore complex promotes H2A.Z incorporation and INO1 transcriptional memory. *Mol. Cell*, **40**, 112–125.
68. Vaucheret,H. (2005) MicroRNA-dependent trans-acting siRNA production. *Sci. STKE*, **2005**, pe43.
69. Qian,W., Miki,D., Zhang,H., Liu,Y., Zhang,X., Tang,K., Kan,Y., La,H., Li,X., Li,S. *et al.* (2012) A histone acetyltransferase regulates active DNA demethylation in Arabidopsis. *Science*, **336**, 1445–1448.
70. Law,J.A., Du,J.M., Hale,C.J., Feng,S.H., Krajewski,K., Palanca,A.M.S., Strahl,B.D., Patel,D.J. and Jacobsen,S.E. (2013) Polymerase IV occupancy at RNA-directed DNA methylation sites requires SHH1. *Nature*, **498**, 385–389.